THE JOURNAL OF PHYSICAL CHEMISTRY A

Article

pubs.acs.org/JPCA

Kinetics of Several Oxygen-Containing Carbon-Centered Free Radical Reactions with Nitric Oxide

Matti P. Rissanen,*[,†] Marvin Ihlenborg,[‡] Timo T. Pekkanen,[§] and Raimo S. Timonen[§]

[†]Department of Physics, University of Helsinki, P.O. Box 64, 00014 Helsinki, Finland

[‡]Department of Chemistry, Institute of Physical Chemistry, University of Kiel, Max-Eyth-Straße 1, 24118 Kiel, Germany

[§]Department of Chemistry, University of Helsinki, P.O. Box 55, 00014 Helsinki, Finland

ABSTRACT: Kinetics of four carbon-centered, oxygen-containing free radical reactions with nitric oxide (NO) were investigated as a function of temperature at a few Torr pressure of helium, employing flow tube reactors coupled to a laser-photolysis/resonance-gas-discharge-lamp photoionization mass spectrometer (LP-RPIMS). Rate coefficients were directly determined from radical (R) decay signals under pseudo-first-order conditions ($[R]_0 \ll [NO]$). The obtained rate coefficients showed negative temperature dependences, typical for a radical−radical association process, and can be represented by the following parametrizations (all in units of cm^3 $molecule^{-1}$ s^{-1}): $k(CH_2OH + NO) = (4.76 \times 10^{-21}) \times (T/300\ K)^{15.92} \times \exp[50700/(RT)]$ (T = 266−363 K, p = 0.79−3.44 Torr); $k(CH_3CHOH + NO) = (1.27 \times 10^{-16}) \times (T/300\ K)^{6.81} \times \exp[28700/(RT)]$ (T = 241−363 K, p = 0.52−3.43 Torr); $k(CH_3OCH_2 + NO) = (3.58 \pm 0.12) \times 10^{-12} \times (T/300\ K)^{-3.17\pm0.14}$ (T = 221−363 K, p = 0.50−0.80 Torr); $k(T)_3 = 9.62 \times 10^{-11} \times (T/300\ K)^{-5.99} \times \exp[-7100/(RT)]$ (T = 221−473 K, p = 1.41−2.95 Torr), with the uncertainties given as standard errors of the fits and the overall uncertainties estimated as ±20%. The rate of CH_3OCH_2 + NO reaction was measured in two density ranges due to its observed considerable pressure dependence, which was not found in the studied hydroxyalkyl reactions. In addition, the CH_3CO + NO rate coefficient was determined at two temperatures resulting in $k_{298K}(CH_3CO + NO) = (5.6 \pm 2.8) \times 10^{-13}$ cm^3 $molecule^{-1}$ s^{-1}. No products were found during these experiments, reasons for which are briefly discussed.

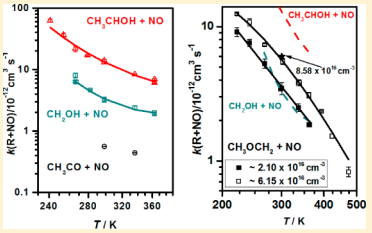

INTRODUCTION

Oxygenated, carbon-centered free radical reactions with nitrogen oxides (NO_x) occur in atmospheric oxidation chemistry[1,2] and in low temperature combustion chemistry.[3,4] The primary oxygenated radicals are formed in the gas phase from volatile oxygen containing organic compounds, such as alcohols and ketones, in hydrogen abstraction reactions by radicals (e.g., ·OH and ·Cl), in thermal decompositions under combustion conditions, and by solar UV photolysis.[1−6] For example, the 1-hydroxyethyl radical (CH_3·CHOH) is the dominant product of OH-initiated ethanol (CH_3CH_2OH) oxidation as the presence of OH-group lowers the α-hydrogen bond dissociation energy.[7−9] The 2-hydroxyethyl radical ($\cdot CH_2CH_2OH$) is the minor product of this reaction, and the abstraction from −OH group is generally found negligible. Methanol oxidation (CH_3OH) in the ambient atmosphere leads mainly to $\cdot CH_2OH$ radicals for the same reasons. The acetyl radical ([CH_3·C(O)] is a common product of many photochemical reactions of ketones, with acetone (CH_3−C(O)CH_3) photolysis being a significant contributor.[10,11] The methoxymethyl radical ($\cdot CH_2OCH_3$) is an important primary radical in the atmospheric dimethyl ether (CH_3OCH_3) oxidation,[12−14] produced by H-abstraction from the ether.

This study includes the reactions of two isomeric but structurally very different C_2H_5O species (CH_3·CHOH and $\cdot CH_2OCH_3$) with nitric oxide and thus supplies important structurally relevant information on the radical reactivity. In addition, the reaction of the smallest hydroxyalkyl radical, $\cdot CH_2OH$, reaction is investigated, and the acetyl radical reaction [CH_3·C(O)] with NO is briefly touched. The previous investigations of these reactions are scarce, with only room temperature rate coefficients reported for the $\cdot CH_2OH$ + NO,[15] CH_3·C(O) + NO[16,17] and for the CH_3·CHOH + NO reaction.[7] To our knowledge there are no previous results for the $\cdot CH_2OCH_3$ + NO reaction.

The search and use of replacements for fossil fuels in combustion engines have the potential to increase ethanol (CH_3CH_2OH)[18,19] (currently the most used biofuel[18]) and dimethyl ether (CH_3OCH_3)[12,20] emissions to the atmosphere. The isomeric C_2H_5O radicals investigated in the current work (i.e., CH_3·CHOH and $\cdot CH_2OCH_3$) are their primary degradation products and are formed from the parent molecules by simple hydrogen abstraction reactions.[7,9,14] Under atmospheric conditions, the reaction with molecular oxygen (O_2) is expected to dominate carbon-centered radical removal due to the very high O_2 concentration and relatively fast rate coefficients.[1,5−7] However, the reactions with NO_x could offer gas-phase synthetic routes to potentially harmful

Special Issue: 100 Years of Combustion Kinetics at Argonne: A Festschrift for Lawrence B. Harding, Joe V. Michael, and Albert F. Wagner

Received: January 31, 2015
Revised: May 5, 2015

ACS Publications © XXXX American Chemical Society

DOI: 10.1021/acs.jpca.5b01027
J. Phys. Chem. A XXXX, XXX, XXX−XXX

and toxic substances and also could potentially affect fuels ignition behavior by affecting the chain branching steps in the reaction mechanism. Thus, the reactivity of these radicals toward nitrogen oxides should be assessed. In a previous publication we have studied reactions of these same radicals with NO_2 under similar conditions,[21] and here we extend the data set to include the NO reactions of these species.

EXPERIMENTAL SECTION

The details of the laser-photolysis/resonance-gas-discharge-lamp photoionization mass spectrometer (LP-RPIMS) apparatus and its data acquisition and analysis have been described in detail previously,[22] and thus, only a brief description of the most relevant details is reported here. The reactions were studied in a 17 mm i.d. tubular stainless-steel flow reactor coated with Halocarbonwax or polydimethylsiloxane (PDMS) and in a 16.5 mm i.d. uncoated Pyrex reactor, under a few Torr pressure (about 0.5−3.5 Torr) of helium bath gas. All the experiments were performed under pseudo-first-order conditions with the molecular reagent nitric oxide (NO) in large excess over the initial radical concentrations produced (i.e., $[R]_0 \ll [NO]$).

The hydrocarbon radical precursor was introduced into the gas flow by bubbling a small, variable part of the bath gas helium through a temperature-controlled liquid precursor reservoir. The concentration in the gas mixture was then estimated from the gas flow rates and the vapor pressures of the pure compounds. The chemicals 1-hydroxy-2-propanone (hydroxyacetone, $CH_3C(O)CH_2OH$, 95%) and 3-hydroxy-2-butanone (acetoine, $CH_3C(O)CHOHCH_3$, 97%) used to produce the hydroxyalkyl radicals ($\cdot CH_2OH$ and $CH_3\cdot CHOH$, respectively) were obtained from Fluka, and 1-methoxy-2-propanone (methoxyacetone, $CH_3C(O)CH_2OCH_3$, 95%) and 3,3-dimethyl-2-butanone (pinacolone, $CH_3C(O)C(CH_3)_3$, 98%) for the $\cdot CH_2OCH_3$ and $CH_3\cdot C(O)$ radical production, respectively, were obtained from Aldrich. The precursor liquids were purified by freeze−pump−thaw cycles. The reagent nitric oxide (NO, Linde, 99.5%) was prepared as described previously[23] and used as a *pure* (~100%) gas. Bath gas helium (He, Messer-Griesheim, 99.9996%) was used as supplied.

The radicals were generated by pulsed ArF exciplex laser photolysis at 193 nm, which for the 1-methoxy-2-propanone (i.e., for the $\cdot CH_2OCH_3$ radical source) can be presented as

$$CH_3C(O)CH_2OCH_3 + h\nu\ (193\ nm) \rightarrow CH_3\cdot C(O) + \cdot CH_2OCH_3 \quad (1)$$

$$CH_3C(O)CH_2OCH_3 + h\nu\ (193\ nm) \rightarrow \text{other products} \quad (2)$$

The ketones used in the current study (see Figure 1) are known to photodissociate by simple C−C bond fission producing acetyl radicals and substituted alkyl radicals (e.g., for hydroxyacetone, $CH_3C(O)CH_2OH + h\nu \rightarrow CH_3\cdot C(O) + \cdot CH_2OH$ [10]) but also potentially have more photolysis pathways accessible at 193 nm than just channel 1. Due to the low initial radical concentrations produced in the laser pulse (i.e., generally close to 10^{11} molecules cm^{-3}), together with the rather high reagent concentration used in the experiments ($[NO] > 10^{12}$ molecules cm^{-3}), the importance of other species produced in the photolysis reaction 2 is considered negligible to the results obtained. The laser pulse energy generating the radicals was varied in some experiments to ensure that the results obtained were independent of this parameter.

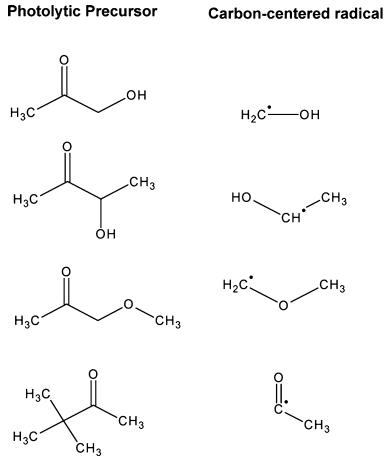

Figure 1. Structures of the photolytic precursors and the corresponding radicals produced.

The decay of the produced radical concentration as a function of time in the flow reactor was measured under varying NO concentrations, and a single-exponential decay was subsequently fitted to the signals obtained, with the decaying time-dependence giving the pseudo-first-order rate coefficient (k') of the investigated reaction. In the beginning and at the end of each experiment, the wall loss rate (k_W) of the radical in the reactor was measured without added NO reagent. The k_W contains all other loss processes of the radical in the reactor except the R + NO reaction and results in a zero-reagent rate shown as one data point in the pseudo-first-order rate plot (Figure 2), with the slope of the plot giving the bimolecular R + NO rate coefficient under those experimental conditions. For the $\cdot CH_2OCH_3$ radical detection, a xenon ionization lamp (8.44 eV) with a sapphire window was used, and for hydroxyalkyl and acetyl radical detections, a chlorine lamp (8.9−9.1 eV) with a calcium fluoride window was used.

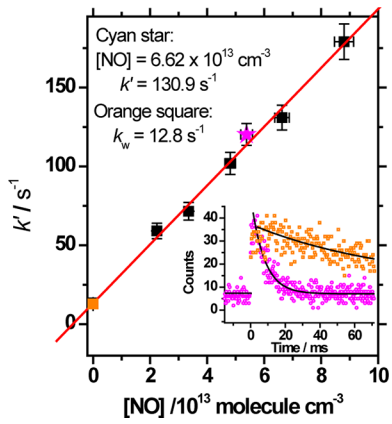

Figure 2. Pseudo-first-order plot of the $\cdot CH_2OCH_3$ + NO reaction, showing the observed first-order radical decay rates (k') as a function of reagent NO concentration of the experiment at 363 K and 0.80 Torr. The insert illustrates the signal decays obtained in the absence (orange) and presence (cyan) of the reagent NO.

The R + NO rate coefficients were determined as a function of temperature and pressure, and the temperature dependences observed were fitted with three commonly applied equations:[24]

DOI: 10.1021/acs.jpca.5b01027
J. Phys. Chem. A XXXX, XXX, XXX−XXX

Table 1. Results and Conditions of the Current R· + NO Experiments [R = ·CH_2OH, CH_3·CHOH, ·CH_2OCH_3, and CH_3·C(O)]

T, K	p/Torr[a] ([He]/10^{16} molecules cm^{-3})	[NO]/10^{13} molecules cm^{-3}	k[b]/10^{-12} cm^3 molecule^{-1} s^{-1}	k_W[c]/s^{-1}	k_W[d]/s^{-1}	laser fluence/mJ cm^{-2}
R = CH_2OH (CH_2OH + NO → Products)[e]						
Below 300 K: $k(T)_2 = [(1.25 \pm 0.22) \times 10^{-14}] \times \exp[(13800 \pm 400)/(RT)]$ cm^3 molecule^{-1} s^{-1}						
Above 295 K: $k(T)_1 = [(3.19 \pm 0.04) \times 10^{-11}] \times (T/300\ \mathrm{K})^{-2.59\pm0.14}$ cm^3 molecule^{-1} s^{-1}						
$k(T)_2 = [(1.92 \pm 0.29) \times 10^{-13}] \times \exp[(7000 \pm 400)/(RT)]$ cm^3 molecule^{-1} s^{-1}						
266−363 K: $k(T)_3 = (4.76 \times 10^{-21}) \times (T/300\ \mathrm{K})^{15.92} \times \exp[50700/(RT)]$ cm^3 molecule^{-1} s^{-1}						
266	0.74 (2.69)	0.39−1.27	8.01 ± 0.78	25.3 ± 3.1	28.9 ± 5.2	11.0
266	3.44 (12.49)	0.48−2.63	6.33 ± 0.23	31.3 ± 1.8	32.3 ± 3.2	13.0
267	2.76 (9.98)	1.12−4.57	6.27 ± 0.39	33.3 ± 1.8	39.8 ± 9.7	17.0
282	2.80 (9.58)	1.14−5.57	4.60 ± 0.12	29.8 ± 0.8	34.0 ± 3.6	17.0
298	0.83 (2.70)	0.47−3.99	3.27 ± 0.22	24.1 ± 1.1	24.4 ± 4.0	12.6
298	3.10 (10.00)	0.62−3.08	3.32 ± 0.23	22.1 ± 0.7	26.6 ± 4.3	17.6
298	3.12 (10.11)	1.03−5.66	3.14 ± 0.14	22.9 ± 1.3	23.3 ± 4.3	9.9
336	3.51 (10.01)	1.68−7.14	2.39 ± 0.15	22.9 ± 1.5	28.3 ± 5.8	11.2
363[f]	0.62 (1.65)	1.22−9.47	1.90 ± 0.06	26.2 ± 1.8	26.8 ± 3.1	
363	3.78 (10.01)	1.08−7.21	1.99 ± 0.05	18.1 ± 1.0	18.7 ± 1.9	15.4
R = CH_3CHOH (CH_3CHOH + NO → Products)[e]						
Below 280 K: $k(T)_2 = [(1.88 \pm 1.10) \times 10^{-15}] \times \exp[(20800 \pm 1200)/(RT)]$ cm^3 molecule^{-1} s^{-1}						
Above 295 K: $k(T)_1 = [(1.31 \pm 0.04) \times 10^{-11}] \times (T/300\ \mathrm{K})^{-3.76\pm0.35}$ cm^3 molecule^{-1} s^{-1}						
$k(T)_2 = [(2.21 \pm 0.78) \times 10^{-13}] \times \exp[(10200 \pm 900)/(RT)]$ cm^3 molecule^{-1} s^{-1}						
241−363 K: $k(T)_3 = (1.27 \times 10^{-16}) \times (T/300\ \mathrm{K})^{6.81} \times \exp[28700/(RT)$ cm^3 molecule^{-1} s^{-1}						
241	2.30 (9.23)	0.16−1.03	62.53 ± 3.25	109.6 ± 5.0	126.5 ± 17.4	18.8
254	2.42 (9.19)	0.46−1.97	36.46 ± 2.51	70.4 ± 3.0	59.2 ± 26.8	20.9
266	2.49 (9.04)	0.45−1.78	21.83 ± 2.52	90.0 ± 21.8	93.2 ± 25.3	5.7
279	2.55 (8.84)	0.43−1.90	16.93 ± 0.46	49.7 ± 1.2	52.7 ± 5.1	12.3
298	0.56 (1.80)	1.01−2.75	12.94 ± 0.40	55.8 ± 1.8	58.4 ± 6.9	18.9
298[f]	2.82 (9.14)	0.85−2.72	14.03 ± 0.55	59.1 ± 1.3	59.4 ± 8.7	
336	3.17 (9.10)	1.01−4.78	8.32 ± 0.17	40.1 ± 0.9	37.8 ± 4.5	15.6
363	0.52 (1.39)	1.94−5.80	6.06 ± 0.13	39.1 ± 1.7	36.5 ± 4.6	18.5
363	3.43 (9.12)	1.26−5.04	6.96 ± 0.21	45.6 ± 1.4	42.5 ± 6.2	18.5
R = CH_3OCH_2, (CH_3OCH_2 + NO → Products)[g]						
At [He] = 2.1 × 10^{16} molecules cm^{-3}:						
$k(T)_1 = [(3.58 \pm 0.12) \times 10^{-12}] \times (T/300\ \mathrm{K})^{-3.17\pm0.14}$ cm^3 molecule^{-1} s^{-1}						
$k(T)_2 = [(2.22 \pm 0.49) \times 10^{-13}] \times \exp[(6900 \pm 500)/(RT)]$ cm^3 molecule^{-1} s^{-1}						
221−363 K: $k(T)_3 = (5.72 \times 10^{-11}) \times (T/300\ \mathrm{K})^{-6.33} \times \exp[-6900/(RT)]$ cm^3 molecule^{-1} s^{-1}						
At [He] = 6.2 × 10^{16} molecules cm^{-3}:						
221−473 K: $k(T)_3 = (9.62 \times 10^{-11}) \times (T/300\ \mathrm{K})^{-5.99} \times \exp[-7100/(RT)]$ cm^3 molecule^{-1} s^{-1}						
221[f]	0.49 (2.12)	0.23−2.32	9.13 ± 0.70	8.3 ± 1.1	13.7 ± 8.9	
221[h]	1.41 (6.16)	0.47−1.43	12.40 ± 0.25	4.2 ± 1.1	6.3 ± 2.1	9.3
241[h]	0.53 (2.12)	0.75−1.99	7.56 ± 0.46	6.5 ± 1.4	4.4 ± 5.80	12.1
241[h,i]	1.54 (6.15)	0.43−1.34	10.78 ± 0.64	5.6 ± 1.0	8.0 ± 5.1	12.1
267[f,h]	0.59 (2.14)	0.49−1.96	5.31 ± 0.44	8.3 ± 1.6	5.3 ± 4.3	
267[f,h]	1.75 (6.34)	0.79−1.61	7.34 ± 0.13	3.2 ± 1.2	3.3 ± 1.2	
298[f,h]	0.65 (2.12)	0.84−4.69	3.45 ± 0.11	10.6 ± 1.0	13.1 ± 2.7	
300[f,h]	0.59 (1.92)	1.01−2.54	3.47 ± 0.36	6.1 ± 1.2	4.5 ± 5.6	
300[f,h]	2.67 (8.58)	1.06−2.11	5.98 ± 0.15	5.2 ± 0.7	6.4 ± 1.9	
302[j]	1.94 (6.20)	0.88−3.73	5.50 ± 0.28	22.7 ± 1.1	29.4 ± 5.4	12.1
336[f,h]	0.74 (2.13)	1.35−6.84	2.49 ± 0.16	17.4 ± 1.0	19.7 ± 6.1	
338[j]	2.08 (5.95)	1.49−4.60	3.83 ± 0.19	23.5 ± 0.9	27.7 ± 5.4	9.0
361[j]	2.25 (6.03)	0.78−5.48	3.09 ± 0.14	18.3 ± 1.2	21.3 ± 4.5	8.8
363[f,h]	0.80 (2.13)	2.24−8.80	1.87 ± 0.05	12.8 ± 1.1	13.3 ± 2.6	
393[j]	2.45 (6.02)	1.91−7.38	2.35 ± 0.03	19.6 ± 0.8	19.2 ± 1.2	9.0
423[j]	2.64 (6.03)	2.51−9.27	1.53 ± 0.06	15.7 ± 1.1	16.0 ± 2.9	7.5
473[j]	2.95 (6.02)	3.79−15.4	0.83 ± 0.07	19.0 ± 1.4	19.5 ± 6.2	9.7
R = CH_3CO (CH_3CO + NO_2 → Products)						
298[f]	2.67 (8.65)	3.13−11.8	0.48 ± 0.02[k]	16.27 ± 0.84	16.03 ± 1.74	
			0.56 ± 0.05[l]		16.24 ± 3.46	
336[f]	3.26 (9.37)	6.60−15.4	0.31 ± 0.02[k]	15.35 ± 0.91	15.64 ± 1.76	
			0.44 ± 0.03[l]		12.64 ± 3.59	

[a] 1 Torr = 133.3 N m^{-2}. [b] Uncertainty stated as 1 standard error of the fit; estimated overall uncertainty in the determined bimolecular rate coefficients is about ±20% (see Figures 3 and 4) except in the CH_3CO + NO reaction, where it was estimated to be about ±50%. [c] Average of measured wall rates. [d] Wall rate determined from y-axis intercept. [e] 17 mm i.d. HalocarbonWax coated reactor and chlorine-lamp with CaF_2 window for photoionization (9.1 eV). [f] Laser pulse energy was not determined during the experiment. [g] Xe/sapphire for photoionization (8.44 eV) unless otherwise stated. [h] 16.5 mm uncoated Pyrex reactor. [i] N-lamp with quartz window (7.1 eV). [j] 17 mm reactor with PDMS coating. [k] The rate coefficient

DOI: 10.1021/acs.jpca.5b01027
J. Phys. Chem. A XXXX, XXX, XXX−XXX

Table 1. continued

obtained from a direct fit to the obtained radical signal. [l]The result when the signal is processed taking into account the apparent production signal at the radical mass (see text).

$$k(T)_1 = k_{300K}(T/300\ \mathrm{K})^n \quad (3)$$

$$k(T)_2 = A\ \exp[-E_A/(RT)] \quad (4)$$

$$k(T)_3 = A'(T/300\ \mathrm{K})^m\ \exp[-E_m/(RT)] \quad (5)$$

where T is temperature in kelvin, R is the gas constant, and k_{300K}, A, A', n, m, E_A, and E_m are empirical parameters obtained from the fits.

The flow tube rate determinations contain several uncertainty sources, which need to be taken into consideration in analyzing the results. The uncertainties mainly arise from uncertainties in reagent concentrations (e.g., uncertainties in flow rates, vapor pressures of the pure compounds, calibration of pressure sensors, etc.) but potentially from other sources too, which were not observed during the experiments but which would not be easily separable from the data obtained. For example, possible contaminants in the reagent NO flow and the generation of other radical products in the photolysis reaction 2 constitute additional potential, though minor, uncertainty factors. By adding the different uncertainty contributions and using the propagation of errors method, the overall uncertainties of the determined reaction rate coefficients were estimated (Table 1).

RESULTS AND DISCUSSION

The determined R + NO rate coefficients and their derived temperature parametrizations are presented in Table 1. The rate coefficients increase with decreasing temperature (see Figure 3 and Figure 4), common to a radical association reaction of the type R + NO → R−NO* (+M) → RNO, with a prereactive complex (R−NO*) on the reaction coordinate.[25,26] Three different parametrizations of the temperature dependence were used (eqs 3−5) in order to adequately account for the observed dependence as well as to supply information for different purposes. The $CH_3{\cdot}C(O)$ + NO reaction was investigated only at two different temperatures, and thus, the temperature parametrizations were not derived.

Due to significant curvature observed in the temperature dependences of the determined rate coefficients [$k(T)$], the commonly applied two-parameter expressions 3 and 4 cannot fully describe the data obtained. In the hydroxyalkyl reactions only the three-parameter eq 5 is able to return a good description of the measured rate coefficients, whereas in the $\cdot CH_2OCH_3$ + NO reaction also the two-parameter expressions produce reasonably good fits for the low pressure data. It should be noted that although there is no real physical reason for using the three-parameter expression [except the curvature in the $k(T)$], and even by inspection it is clear that the parameters obtained vary much for results that are comparable in magnitude, yet the given parametrizations were found to give the best description of the current results. Only the parametrizations that were found to give a reasonable fit are given in Table 1. For example, one Arrhenius parametrization is able to describe the temperature dependence of the $\cdot CH_2OCH_3$ + NO reaction at the lower density range quite well, and thus, only one parametrization is given, whereas for the results obtained at the higher density range with a broader experimental temperature range, two different Arrhenius

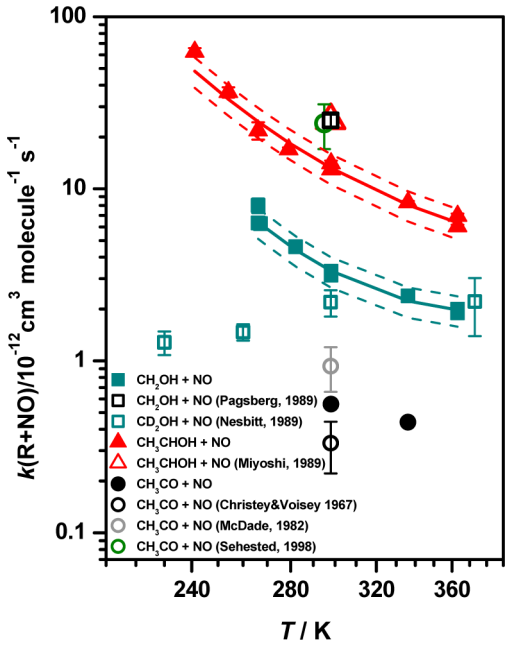

Figure 3. Determined rate coefficients of the $\cdot CH_2OH$, $CH_3{\cdot}CHOH$, and $CH_3{\cdot}C(O)$ reactions with NO shown as a function of temperature. The overall uncertainty of the obtained rate coefficients was estimated as ±20%, and the dashed lines indicate the variation of k between these limits. Also included are the previous results by Pagsberg et al.[15] for the $\cdot CH_2OH$ + NO reaction, by Nesbitt et al.[27] for the closely related $\cdot CD_2OH$ + NO reaction, by Miyoshi et al.[7] for the $CH_3{\cdot}CHOH$ + NO reaction, and by McDade et al.,[17] Christey and Voisey,[28] and Sehested et al.[16] for the $CH_3{\cdot}C(O)$ + NO reaction.

parametrizations would be needed to describe the data obtained. Furthermore, the three-parameter fitting procedure returned unrealistic error limits (e.g., bigger uncertainty value than the corresponding parameter value, which would imply a negative rate coefficient), and thus, only the estimated overall uncertainties for these fits are reported (Table 1). In addition, the variation of the rate coefficients within these estimated limits are indicated by dashed lines in Figures 3 and 4.

The activation energy (E_A) of the Arrhenius equation (eq 4) is not generally applicable for reactions with submerged barriers on the potential energy surface (i.e., reactions with apparent negative activation energies), but the Arrhenius parameters were nevertheless determined in order to enable easier comparison with previous results. As noted above, using only two parameters resulted in poor expression for the determined temperature dependences especially in the case of the hydroxyalkyl reactions, with significant deviation from the measured rate coefficients in the extremes of the experimental temperature range. However, the temperature dependences can be better described in the Arrhenius form by dividing the experimental temperature range into two different regimes, each with different parametrization. Thus, the obtained hydroxyalkyl rate coefficients were arbitrarily divided into two different temperature ranges which resulted in the parametrizations given in Table 1. The curvature and change in the apparent activation energy potentially indicate another reaction channel becoming important as the temperature

DOI: 10.1021/acs.jpca.5b01027
J. Phys. Chem. A XXXX, XXX, XXX−XXX

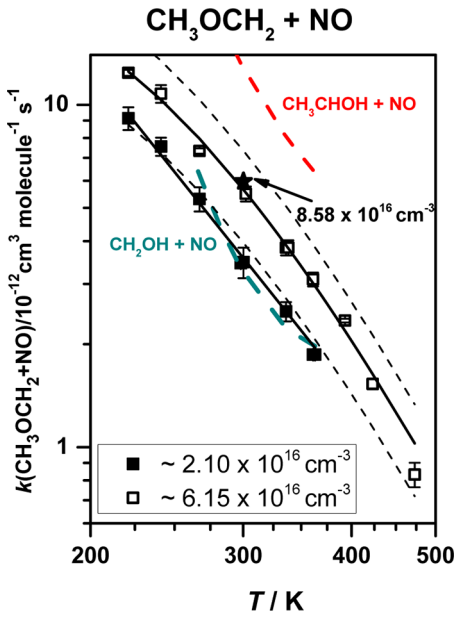

Figure 4. Determined $\cdot CH_2OCH_3$ + NO reaction rate coefficients shown as a function of temperature at two different bath gas densities (Table 1). The density change of about a factor of 3 increases the reaction rate coefficient roughly about 50%. The single value determined at the highest density and shown with a star symbol has been omitted from the fits. The overall uncertainty of the obtained rate coefficients was estimated as ±20%, and the dashed lines indicate the variation of k between these limits for the results obtained at the higher density range. Also included are the fits obtained for the $\cdot CH_2OH$ + NO and $CH_3\cdot CHOH$ + NO reactions.

changes, but unfortunately with no products found (as will be dealt more thoroughly below), this hypothesis cannot be proven or rejected.

The thing that is striking from the obtained $k(T)$ parameters is the very steep temperature dependences, much stronger than what were previously obtained for the same radicals in their corresponding R + NO_2 reactions.[21] Furthermore, in the hydroxyalkyl reactions the observed temperature dependences are significantly stronger at colder temperatures, an observation that could indicate pronounced reactivity on the reactor surfaces in a cooler reactor. Though somewhat higher wall rates were measured at cooler conditions, especially in the $CH_3C\cdot HOH$ + NO reaction where also the steepest temperature dependence was observed (Table 1 and Figure 3), the determined bimolecular rate coefficients cannot be explained by increasing surface reactions as the wall rate was measured in each experiment and is included in the rate coefficient analysis (see Figure 2). Thus, the increase must be due to a gas-phase process. Moreover, the same combination of radical precursor, reactor, and photolysis production was used in our previous R + NO_2 study[21] with no indication of enhanced rate coefficients at colder temperatures.

In the $\cdot CH_2OCH_3$ + NO reaction also a significant pressure dependence was observed (see Figure 4), with the determined rate coefficients increasing by about 35−65% with a factor of 3 increase in bath gas density, the relative increase being more at higher temperatures. The investigated hydroxyalkyl reactions did not show significant changes in the rates when the bath gas helium pressure was varied at around 0.5−3.5 Torr.

Due to the missing absorption coefficients and quantum yields for the radical precursor compounds at the 193 nm laser photolysis wavelength, it is not possible to calculate the initial radical concentrations used in these experiments. However, it is possible to use indirect indicators of the concentration produced, the concentration range being crucial for the rate determination by the pseudo-first-order rate method. These indicators include, for example, the linearity of the obtained pseudo-first-order rate plots and the single-exponential decay behavior of the radical signals observed, especially the radical decays observed in absence of NO (see Figure 2). In addition, the variation of the laser power in the experiments did not cause noticeable changes in the obtained rate coefficients, and thus, the results obtained in the current study are not affected by second-order radical processes to any significant extent.

Products of the reactions were sought with different photoionization energies, but no unambiguous product identification could be made. The R + NO radical association reaction is thought of leading to nitroso compounds (i.e., RNO), provided that the bath gas collisions are enough to stabilize the nascent R−NO* collision complexes at the low pressures of the current experiments. Indeed it seems that these association products were formed in the studied reactions with significant yields but were potentially photodissociated during photoionization. This was indicated by the primary radical signals (e.g., $\cdot CH_2OCH_3$ signals in the $\cdot CH_2OCH_3$ + NO investigation), when higher ionization energies were applied (i.e., higher than in normal rate measurements performed with xenon and chlorine lamps, 8.44 and 9.1 eV, respectively), resulting in "an equilibrium type of signal" that does not decay to the prephotolysis background signal level during the reaction time (cf. ref 23, a_0 in Figure 5). This strongly suggests that a

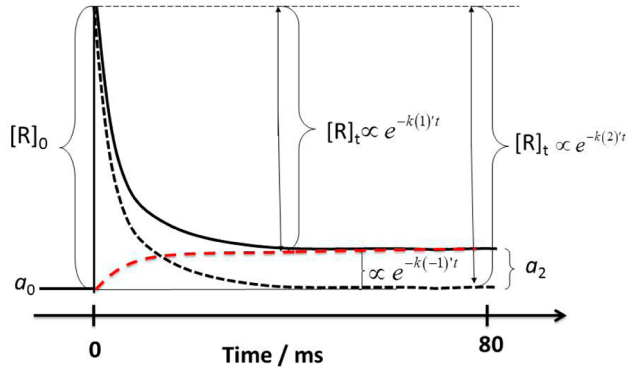

Figure 5. Schematic of the obtained radical signal explaining the fitting routines used to analyze the $CH_3\cdot C(O)$ radical decays. In the figure, a_0 is the prephotolysis background signal level, $[R]_0$ is the initial radical concentration produced in the laser pulse, $[R]_t$ is the radical concentration after reaction time t and is dependent on the pseudo-first-order rate coefficient $k(x)'$ of the reaction. In the experiments a baseline shift a_2 was observed and thus a double-exponential function was fitted to the $CH_3\cdot C(O)$ radical signal (see text).

fragment with a similar mass as NO (i.e., m/z = 30 Th) is lost from the parent ion (RNO^+) subsequent to photoionization. This type of result has been obtained for a few other R + NO reactions measured in our setup, and the radical decay has been returned to "a normal type of behavior" (i.e., R decay to the prephotolysis background; Figure 2) by using lower ionization energies. The nitroso compounds are generally expected to have relatively low R−NO bond energies, which may result in an equilibrium in the reaction (i.e., R + NO ↔ RNO) at correspondingly low temperatures,[3,23] though for the saturated

DOI: 10.1021/acs.jpca.5b01027
J. Phys. Chem. A XXXX, XXX, XXX−XXX

radicals of the current study the equilibrium behavior is not expected at least below 450 K.

A similar type of "false-equilibrium" signal was observed in the $CH_3{\cdot}C(O)$ + NO radical reaction, again likely due to the use of too high ionization energy (9.1 eV), which was nevertheless necessary in order to obtain good enough signals to perform the rate experiments. By analogy to other R + NO reactions,[3,23] the $CH_3{\cdot}C(O)$ + NO reaction is not expected to show equilibrium behavior at such low temperatures as used in the current study. An example of the observed signal profile and the two different methods of fitting are shown in Figure 5. In the first method a single-exponential decay curve was fitted directly to the raw ion signal without taking into consideration the observed shift in the prephotolysis background (marked as a_2 in Figure 5). In the second method a double-exponential function was fitted to the obtained signal by assuming that the apparent formation rate (i.e., the reason why the signal does not decay to the background) is due to a photofragmentation process during ionization and thus has exactly the same time behavior and can be fixed as $k(1)' = k(-1)'$. The amplitudes of the exponentials can be read from the obtained signal (i.e., $[R]_0$ and a_2 in Figure 5, for example), and by fixing the amplitudes and constraining the reverse rate equal to the forward rate, the corrected $k(1)'$ could be retrieved. This procedure led to about 25% higher rate coefficients. The rate coefficients according to both procedures are given in Table 1.

A reaction mechanism analogous to that observed in the $\cdot CH_2OH + O_2$ reaction,[29] with a prereactive complex on the reaction coordinate and in the case of the $\cdot CH_2OH$ + NO reaction leading to HCHO + HNO products (and to CH_3CHO + HNO in $CH_3{\cdot}CHOH$ + NO reaction), could explain the apparent negative activation energies and the lack of pressure dependence obtained. However, we sought for the corresponding aldehyde species in each reaction by applying different ionization energies but did not detect them. From previous works we know that the RPIMS used in this work is fairly sensitive to these carbonyl compounds, and thus, it is unlikely that they were formed in these reactions with a significant yield. We have not been able to detect previously the coproduct HNO despite considerable effort invested, potentially due to absence of suitable photoionization lines within our photoionization setup, resulting in photodissociation in the photoionizator (as was also discussed above for the potential organo nitroso products). Another conceivable possibility for unsuccessful detection could be that the aldehyde species were fragmented due to excitation obtained from the exothermic R + NO reactions. However, in the absence of detected reaction products, the actual reaction mechanisms can only be speculated.

Previous rate coefficient determinations for the reactions investigated are scarce. The $\cdot CH_2OH$ + NO reaction was studied previously by Pagsberg et al.[15] at 298 K and at atmospheric pressure of argon (Ar) using F· + CH_3OH reaction for radical generation and UV absorption for direct detection of the $\cdot CH_2OH$ radical. They obtained $(2.5 \pm 0.2) \times 10^{-11}$ cm^3 molecule^{-1} s^{-1}, a vastly different value than what is determined in the current work $(3.71 \pm 0.13) \times 10^{-12}$ cm^3 molecule^{-1} s^{-1}. However, the pulse radiolysis technique used by Pagsberg et al.[15] creates free radicals in a less controllable and unselective fashion than the direct laser photolysis used in this work. Pagsberg et al. also employed much higher reagent (and thus also radical) concentrations in their experiments and correspondingly shorter reaction monitoring time-scale on the order of microseconds, which could result in contribution of excited species to the observed kinetics. In the current work the reactions were studied in tens of milliseconds reaction time (see Figure 2), with the first millisecond always omitted from the analysis to exclude possible excited species contribution. Thus, it is concluded that the discrepancy between the reported values could result from the different radical production method in the work of Pagsberg et al.[15] in comparison with the current investigation.

The analogous reaction of the isotopologue $\cdot CD_2OH$ with NO was studied as a function of pressure and temperature (p = 0.5−1.5 Torr of He, T = 230−373 K) by Nesbitt et al.[27] using discharge-flow/mass spectrometry apparatus and found a pressure independent rate coefficient of $k_{298K}(\cdot CD_2OH + NO) = (2.2 \pm 0.4) \times 10^{-12}$ cm^3 molecule^{-1} s^{-1}. The value determined at room temperature is in relatively good agreement with the result obtained in this study and consistent with the proposed complex association decomposition mechanism, provided that the α-hydrogens do not take part in the primary reaction step (i.e., only secondary kinetic isotope effect affecting the rate coefficient). However, the temperature dependence obtained by Nesbitt et al.[27] is opposite to what is found here (see Figure 3). Though the discrepancy between the obtained results cannot be reconciled based on the available documentation, it should be noted that a similar discrepancy (i.e., positive vs negative apparent activation energy) was also observed in the $CH_2OH + O_2$ reaction rate coefficients determined by Nesbitt et al.,[30] in contrast with more recent experimental and theoretical work.[29]

The other hydroxyalkyl reaction investigated, $CH_3C{\cdot}HOH$ + NO, has been studied previously by Miyoshi et al.[7] at 295 K and at a few Torr of He. They used similar methods as in the current study and obtained $(2.41 \pm 0.60) \times 10^{-11}$ cm^3 molecule^{-1} s^{-1}. The rate coefficient was determined only at room temperature and is in reasonable agreement with the $k_{298K}(CH_3{\cdot}CHOH + NO) = (1.38 \pm 0.07) \times 10^{-11}$ cm^3 molecule^{-1} s^{-1} determined in the current work (see Table 1 and Figure 3).

The $CH_3{\cdot}C(O)$ + NO rate coefficient has been determined by Sehested et al.[16] at 295 K and 1 atm of SF_6, employing pulse radiolysis/UV−vis absorption method, and by McDade et al.[17] at 298 K and at a few Torr of He using similar LP-RPIMS method as used in the current work. Sehested et al.[16] obtained $k_{295K}(CH_3{\cdot}C(O) + NO) = (2.4 \pm 0.7) \times 10^{-11}$ cm^3 molecule^{-1} s^{-1}, a much higher value than obtained in this work [$k_{298K}(CH_3{\cdot}C(O) + NO) = (4.8 \pm 2.4) \times 10^{-13}$ cm^3 molecule^{-1} s^{-1} and $k_{298K}(CH_3{\cdot}C(O) + NO)_{CORRECTED} = (5.6 \pm 2.8) \times 10^{-13}$ cm^3 molecule^{-1} s^{-1}], whereas McDade et al.[17] obtained $k_{298K}(CH_3{\cdot}C(O) + NO) = (9.3 \pm 2.7) \times 10^{-13}$ cm^3 molecule^{-1} s^{-1}, much closer to the current result. In addition, a previous estimation of the $CH_3{\cdot}C(O)$ + NO rate coefficient was made by Christie and Voisey[28] by fitting to a complex reaction system and finding a value of $k_{298\ K}(CH_3{\cdot}C(O) + NO) = 3.32 \times 10^{-13}$ cm^3 molecule^{-1} s^{-1}, in good agreement with the values determined in the current study. By comparing the results obtained in the current and previous works, it seems that the studies performed with the pulse radiolysis radical generation method have significantly overestimated the rate coefficients, potentially due to the combined effects of complex reaction mixture and relatively high radical concentration inherent with the technique, as was already noted above in the case of $\cdot CH_2OH$ + NO reaction. There are no previous results for the $\cdot CH_2OCH_3$ + NO reaction, and thus, a similar comparison

DOI: 10.1021/acs.jpca.5b01027
J. Phys. Chem. A XXXX, XXX, XXX−XXX

cannot be performed. The determined rate coefficients are presented in Figures 3 and 4 together with the previously reported values.

The reactivity of the studied radicals toward NO is quite different from their previously observed reactivity in the corresponding R· + NO_2 reactions[21] (Table 2). All these radicals show less reactivity toward NO than NO_2, only the CH_3·CHOH radical approaching the high reactivity observed in its R· + NO_2 reaction. Most notably the reactivity order is different, being (in the R· + NO reactions) roughly $k_{298K}(CH_3·CHOH) > k_{298K}(·CH_2OCH_3) \sim k_{298K}(·CH_2OH) > k_{298K}(CH_3·C(O))$, whereas in the R· + NO_2 reactions the reactivities at 298 K are[21] $k_{298K}(·CH_2OH) > k_{298K}(·CH_2OCH_3) \sim k_{298K}(CH_3·CHOH) > k_{298K}(CH_3·C(O))$. Especially the ·$CH_2OH$ and ·CH_2OCH_3 radicals are significantly less reactive toward NO than NO_2. As in the analogic R· + NO_2 reactions, the CH_3·C(O) radical is the least reactive radical in the group, with about 2 orders of magnitude smaller rate coefficient with NO than with NO_2.

Table 2. Current R· + NO and Previous R· + NO_2 [21] Room Temperature (T = 298 K) Rate Coefficients for R = ·CH_2OH, CH_3·CHOH, ·CH_2OCH_3, and CH_3·C(O)

radical R·	k_{298K}(R· + NO)/10^{-12} cm^3 molecule^{-1}s^{-1}	k_{298K}(R· + NO_2)/10^{-12} cm^3 molecule^{-1}s^{-1}
·CH_2OH	3.3	89.5
CH_3·CHOH	13.2	74.8
·CH_2OCH_3	3.5[a]	78.5
CH_3·C(O)	0.6	28.7

[a]Value at about 0.6 Torr of helium bath gas; note that the ·CH_2OCH_3 + NO reaction rate coefficient is pressure dependent.

As has been commonly found in previous carbon-centered free radical reaction investigations, the reactivity differences observed between the studied oxygenated radicals toward a common reagent can likely be explained by the inductive effects of the substituents connected to the radical center carbon atom, enhancing or decreasing the rate of reaction by increasing or decreasing the electron density in the radical center.[31−33] Electropositive alkyl substitution at the radical carbon (e.g., the extra methyl group in CH_3·CHOH in comparison with ·CH_2OH) enhances the R· + NO reaction rate, whereas with the electronegative methoxy substitution in the radical carbon (i.e., −OCH_3 in ·CH_2OCH_3) the reaction rate does not change much from the ·CH_2OH + NO reaction, indicating that the electronegative methoxy and hydroxyl substituents affect the observed reactivity in R· + NO reaction about equally. The CH_3·C(O) radical is somewhat of an outlier as far as the structure goes (Figure 1), and thus, the comparison might be less meaningful. It is possible, however, that the much lower reactivity is caused by the electronegative carbonyl group pulling away the electron density from the radical center.

The measured R· + NO rate coefficients are comparable to their corresponding R· + O_2 rate coefficients,[7,29,34] and thus, the loss of these radicals from an atmospheric gas mixture is dominated by reaction with O_2, the reactions with NO and NO_2 being of minor importance.

CONCLUSIONS

Several oxygenated free radical reactions with NO were studied in low pressure flow tube experiments using photoionization mass spectrometry for direct radical detection. The determined rate coefficients showed negative temperature dependence, typical for a complex radical−radical association process. In the ·CH_2OCH_3 + NO reaction, also a pressure dependence was observed, whereas in the CH_3·C(O), CH_3·CHOH, and ·CH_2OH reactions the determined rate coefficients did not indicate any significant pressure dependence. The reactivity differences between the studied reactions were tentatively proposed to result from different charge distributions at the radical center carbon atom, based on the structures of the radicals and their measured rate coefficients with NO. The results of the study increase our knowledge on oxygenated carbon-centered free radical reactions with NO, for which a relatively scarce database exists up to date.

AUTHOR INFORMATION

Corresponding Author

*E-mail: matti.p.rissanen@helsinki.fi. Phone: +358458730170.

Notes

The authors declare no competing financial interest.

REFERENCES

(1) Atkinson, R.; Baulch, D. L.; Cox, R. A.; Crowley, J. N.; Hampson, R. F.; Hynes, R. G.; Jenkin, M. E.; Rossi, M. J.; Troe, J. Evaluated Kinetic and Photochemical Data for Atmospheric Chemistry: Volume I - Gas Phase Reactions of O_x, HO_x, NO_x and SO_x Species. *Atmos. Chem. Phys.* **2004**, *4*, 1461−1738.

(2) Wayne, R. P. *Chemistry of Atmospheres*, 3rd ed.; Oxford University Press, Inc.: New York, 2000.

(3) Miller, J. A.; Bowman, C. T. Mechanism and Modeling of Nitrogen Chemistry in Combustion. *Prog. Energy Combust. Sci.* **1989**, *15*, 287−338.

(4) Miller, J. A.; Pilling, M. J.; Troe, J. Unravelling Combustion Mechanisms through a Quantitative Understanding of Elementary Reactions. *Proc. Combust. Inst.* **2005**, *30*, 43−88.

(5) Monks, P. S. Gas-phase Radical Chemistry in the Troposphere. *Chem. Soc. Rev.* **2005**, *34*, 376−395.

(6) Sander, S. P.; Friedl, R. R.; Abbat, J. P. D.; Barker, J. R.; Burkholder, J. B.; Golden, D. M.; Kolb, C. E.; Kurylo, M. J.; Moortgat, G. K.; Wine, P. H.; et al. Chemical Kinetics and Photochemical Data for Use in Atmospheric Studies: Evaluation Number 17. Publication 10-06; National Aeronautics and Space Administration, Jet Propulsion Laboratory, California Institute of Technology: Pasadena, CA, 2011.

(7) Miyoshi, A.; Matsui, H.; Washida, N. Reactions of Hydroxyethyl Radicals with Oxygen and Nitric Oxide. *Chem. Phys. Lett.* **1989**, *160*, 291−294.

(8) Grosjean, D. Atmospheric Chemistry of Alcohols. *J. Braz. Chem. Soc.* **1997**, *8*, 433−442.

(9) Carr, S. A.; Blitz, M. A.; Seakins, P. W. Site-Specific Rate Coefficients for Reaction of OH with Ethanol from 298 to 900 K. *J. Phys. Chem. A* **2011**, *115*, 3335−3345.

(10) Wu, Y.; Xie, D.; Xue, Y. Ab Initio Studies for the Photodissociation Mechanism of Hydroxyacetone. *J. Comput. Chem.* **2003**, *24*, 931−938.

(11) Blitz, M. A.; Heard, D. E.; Pilling, M. J. Study of Acetone Photodissociation over the Wavelength Range 248−330 nm: Evidence of a Mechanism Involving Both the Singlet and Triplet Excited States. *J. Phys. Chem. A* **2006**, *110*, 6742−6756.

(12) Herrmann, F.; Oßwald, P.; Kohse-Höinghaus, K. Mass Spectrometric Investigation of the Low-Temperature Dimethyl Ether Oxidation in an Atmospheric Pressure Laminar Flow Reactor. *Proc. Combust. Inst.* **2013**, *34*, 771−778.

(13) Good, D. A.; Francisco, J. S. Tropospheric Oxidation Mechanism of Dimethyl Ether and Methyl Formate. *J. Phys. Chem. A* **2000**, *104*, 1171−1185.

(14) Carr, S. A.; Still, T. J.; Blitz, M. A.; Eskola, A. J.; Pilling, M. J.; Seakins, P. W.; Shannon, R. J.; Wang, B.; Robertson, S. H. Experimental and Theoretical Study of the Kinetics and Mechanism

DOI: 10.1021/acs.jpca.5b01027
J. Phys. Chem. A XXXX, XXX, XXX−XXX

of the Reaction of OH Radicals with Dimethyl Ether. *J. Phys. Chem. A* **2013**, *117*, 11142−11154.
(15) Pagsberg, P.; Munk, J.; Anastasi, C.; Simpson, V. J. Reaction of CH_2OH with O_2, NO, and NO_2 at Room Temperature. *J. Phys. Chem.* **1989**, *93*, 5162−5165.
(16) Sehested, J.; Christensen, L. K.; Nielsen, O. J.; Wallington, T. J. Absolute Rate Constants for F + CH_3CHO and CH_3CO + O_2, Relative Rate Study of CH_3CO + NO, and the Product Distribution of the F + CH_3CHO Reaction. *Int. J. Chem. Kinet.* **1998**, *30*, 913−921.
(17) McDade, C. E.; Lenhardt, T. M.; Bayes, K. D. The Rate of Reaction of Acetyl and Benzoyl Radicals with O_2. *J. Photochem.* **1982**, *20*, 1.
(18) Goldemberg, J.; Guardabassi, P. Are Biofuels a Feasible Option? *Energy Policy* **2009**, *37*, 10−14.
(19) Kirstine, W. V.; Galbally, I. E. The Global Atmospheric Budget of Ethanol Revisited. *Atmos. Chem. Phys.* **2012**, *12*, 545−555.
(20) Semelsberger, T. A.; Borup, R. L.; Greene, H. L. Dimethyl Ether (DME) as an Alternative Fuel. *J. Power Sources* **2006**, *156*, 497−511.
(21) Rissanen, M. P.; Arppe, S. L.; Timonen, R. S. Kinetics of Several Oxygenated Carbon-Centered Free Radical Reactions with NO_2. *J. Phys. Chem. A* **2013**, *117*, 3902−3908.
(22) Eskola, A. J.; Timonen, R. S. Kinetics of the Reactions of Vinyl Radicals with Molecular Oxygen and Chlorine at Temperatures 200-362 K. *Phys. Chem. Chem. Phys.* **2003**, *5*, 2557−2561.
(23) Rissanen, M. P.; Amedro, D.; Krasnoperov, L.; Marshall, P.; Timonen, R. S. Gas Phase Kinetics and Equilibrium of Allyl Radical Reactions with NO and NO_2. *J. Phys. Chem. A* **2013**, *117*, 793−805.
(24) Smith, I. W. M. The Temperature-Dependence of Elementary Reaction Rates: Beyond Arrhenius. *Chem. Soc. Rev.* **2008**, *37*, 812−826.
(25) Mozurkewich, M.; Benson, S. W. Negative Activation Energies and Curved Arrhenius Plots. 1. Theory of Reactions over Potential Wells. *J. Phys. Chem.* **1984**, *88*, 6429−6435.
(26) Troe, J. The Colourful World of Complex-Forming Bimolecular Reactions. *J. Chem. Soc. Faraday Trans.* **1994**, *90*, 2303−2317.
(27) Nesbitt, F. L.; Payne, W. A.; Stief, L. J. Kinetic Studies of the Hydroxymethyl Radical with NO and NO_2. *J. Phys. Chem.* **1989**, *93*, 5158−5161.
(28) Christie, M. I.; Voisey, M. A. Reactions of Acetyl Radicals. Part 2. Reaction of Acetaldehyde with Nitrogen Dioxide in Presence of Nitric Oxide. *Trans. Faraday Soc.* **1967**, *63*, 2702.
(29) Schocker, A.; Uetake, M.; Kanno, N.; Koshi, M.; Tonokura, K. Kinetics and Rate Constants of the Reaction $CH_2OH + O_2 \rightarrow CH_2O + HO_2$ in the Temperature Range of 236-600 K. *J. Phys. Chem. A* **2007**, *111*, 6622−6627.
(30) Nesbitt, F. L.; Payne, W. A.; Stief, L. J. Temperature Dependence for the Absolute Rate Constant for the Reaction $CH_2OH + O_2 \rightarrow HO_2 + H_2CO$ from 215 to 300 K. *J. Phys. Chem.* **1988**, *92*, 4030−4032.
(31) Marston, G.; Monks, P. S.; Wayne, R. P. In *General Aspects of the Chemistry of Radicals*; Alfassi, Z. B., Ed.; John Wiley & Sons Ltd.: New York, 1999; pp 429−471.
(32) Paltenghi, R.; Ogryzlo, E. A.; Bayes, K. D. Rates of Reaction of Alkyl Radicals with Ozone. *J. Phys. Chem.* **1984**, *88*, 2595−2599.
(33) Timonen, R. S.; Gutman, D. Kinetics of the Reactions of Methyl, Ethyl, Isopropyl, and tert-Butyl Radicals with Molecular Chlorine. *J. Phys. Chem.* **1986**, *90*, 2987−2991.
(34) Rosado-Reyes, C. M.; Francisco, J. S.; Szente, J. J.; Maricq, M. M.; Frøsig Østergaard, L. Dimethyl ether oxidation at elevated temperatures (295-600 K). *J. Phys. Chem. A* **2005**, *109*, 10940−10953.

DOI: 10.1021/acs.jpca.5b01027
J. Phys. Chem. A XXXX, XXX, XXX−XXX